ELSEVIER

Materials Science and Engineering A273–275 (1999) 457–461

MATERIALS SCIENCE & ENGINEERING A

www.elsevier.com/locate/msea

Formation of a nanocrystalline structure during direct and reverse martensitic transformations

V.V. Sagaradze *, I.G. Kabanova

Institute of Metal Physics, Ural Branch RAS, 18 S.Kovalevskaya Str., 620219 Ekaterinburg, Russia

Abstract

We studied different methods employing direct and reverse $\gamma \rightarrow \alpha^1 \rightarrow \gamma$ transformations for producing a fine fcc structure in austenitic steels alloyed with Ni, Cr or Ti. Finest nanodimensional austenitic crystals were obtained not by fast heating during the $\alpha^1 \rightarrow \gamma$ transformation (or subsequent recrystallization) but by slow heating at a rate of 0.2–0.4 K min^{-1}, when multiplication of γ-crystallite orientations occurred. The electron microscopy showed that $24^2 = 576$ orientations of the γ-phase appeared in each initial austenitic grain during a single cycle of $\gamma \rightarrow \alpha^1 \rightarrow \gamma$ transformations. Crystallographic calculations of all possible misorientations of any adjacent γ-crystals having the Kurdyumov–Sachs relationship suggested that a limited number (approximately 10.5, 49.5, 60°, etc.) of unlike misorientation angles was formed. The nanocrystalline state and predominance of large-angle boundaries between fine γ-crystals account for a very strong strengthening of the steels. This may be used in practical applications.

Keywords: Martensite; Austenitic steels; Misorientation angles; Nanocrystalline microstructure

1. Introduction

The formation of the ultrafine or nanocrystalline structural state provides new approaches to radical improvement of mechanical and physical properties of many metallic materials [1]. The structure of materials is usually refined during deposition of elements from the gaseous or liquid phase, crystallization of amorphous metal alloys, or as a result of a strong plastic deformation. This study deals with a nontraditional method of formation of a submicrocrystalline structure in metastable austenitic alloys during direct and reverse martensitic $\gamma \rightarrow \alpha^1 \rightarrow \gamma$ transformations [2–4]. Under certain treatment conditions [5] this cyclic martensitic transformation leads to a progressive multiplication of γ-orientations (up to $24^2 = 576$) and causes strong refinement of the structure. This paper focuses on the analysis of the conditions necessary to produce the nanocrystalline austenitic state, determination of all possible misorientation angles of γ-crystals, and estimation of mechanical properties of such metastable Fe–Ni-based alloys.

* Corresponding author. Fax: +7-3432-740003.
E-mail address: rdnr@neutron.e-burg.su (V.V. Sagaradze)

2. Materials and methods

The subjects of study were metastable austenitic alloys types 32Ni (Fe–32.3wt.%Ni) and 26Ni–Cr–Ti (Fe–26wt.%Ni–1.3wt.%Cr–1.5wt.%Ti), which have the martensite transformation start temperature M_s at 183 and 144 K, respectively. The phase and crystallographic analyses of the alloy samples were performed using the transmission electron microscopy technique.

3. Results and discussion

3.1. Formation of the nanostructure during the $\gamma \rightarrow \alpha^1 \rightarrow \gamma$ transformation

The 32Ni and 26Ni–Cr–Ti alloys [4,5] quenched from 1323 K possess a polyhedral austenitic structure with a grain size of 30–50 μm. Cooling in liquid nitrogen causes the direct martensitic $\gamma \rightarrow \alpha^1$ transformation, leading to a volume fractionof about 90 and 65% of the lenticular martensite having 24 orientations and the habit $\{3.10.15\}_\gamma$ (Fig. 1a), respectively. If the reverse martensitic $\alpha^1 \rightarrow \gamma$ transformation is realized during heating up to 973 K at a rate exceeding 3 K

0921-5093/99/$ - see front matter
PII: S0921-5093(99)00327-5

min^{-1}, the dimensions and the shape of the initial austenitic grain are preferably restored and a small number of thin γ twins is formed [5]. These generally accepted conditions of treatment do not lead to a marked refinement of the initial austenitic structure, a fact which is due to the nucleation of the γ-phase at the boundary with the retained austenite and to the reproduction of its orientation. To ensure that 24 orientations of the γ-phase nucleate inside each martensitic α-crystal during heating and the γ orientations multiply during the $\gamma \rightarrow \alpha^1 \rightarrow \gamma$ cycle, one should provide a low-nickel 'buffer' layer at the boundaries of the martensitic α^1-crystals [6]. This layer inhibits the nucleation and growth of the γ-phase on the retained austenite as on a substrate. The low-nickel buffer layer may be formed through a redistribution of nickel between the martensite and the austenite in accordance with the equilibrium diagram of the Fe–Ni system under very slow heating, which provides conditions for a considerable diffusion of nickel from the surface layers of the martensitic α^1-crystals to the retained austenite. Calculations show [6] that at 670 K (holding time of 10 h) a layer containing $\leq$25wt.% nickel and about 1 nm deep is formed at the boundaries of martensitic crystals. In this nickel-depleted region the temperature of the reverse martensitic $\alpha^1 \rightarrow \gamma$ transformation is much higher than in the central regions of the α^1-crystals containing 32.3% nickel. For this reason, during the $\alpha^1 \rightarrow \gamma$ transformation the austenite does not nucleate at the boundary with the retained austenite nor restores its initial orientation: it appears inside the martensitic lens and forms all the 24 γ-orientations that are possible.

After the $\gamma \rightarrow \alpha^1 \rightarrow \gamma$ transformation cycle $24^2 = 576$ orientations of the γ-phase may appear. If coinciding orientations are taken into account, 501 different orientations of the γ-phase [7] may be formed in each initial γ-grain after a single cycle of the $\gamma \rightarrow \alpha^1 \rightarrow \gamma$ transformations for the Kurdyumov–Sachs orientation relationships. Fig. 1b shows superthin crystals of the γ-phase, which were formed as a result of the $\gamma \rightarrow \alpha^1 \rightarrow \gamma$ transformation in the 32Ni alloy. The reverse $\alpha^1 \rightarrow \gamma$ transformation was performed during slow heating at a rate of 0.3 K min^{-1}. Depending on particular conditions of the $\alpha^1 \rightarrow \gamma$ transformation, the γ-crystals may be 10–50 nm thick, a value which is several orders of magnitude lower than the dimensions of the initial austenitic grains (30–50 μm or larger). In the 26Ni–Cr–Ti alloy superfine austenitic crystals may also be formed during the isothermal $\alpha^1 \rightarrow \gamma$ transformation at 813 K (Fig. 1c). Typical diffraction patterns for all the 24 orientations of the γ-phase in the initial α^1-crystal appear (Fig. 1d). At the beginning of the martensitic $\alpha^1 \rightarrow \gamma$ transformation fine γ-crystals have a coherent bcc/fcc interphase boundary. Then the coherence is disturbed and the γ-crystals of 24 orientations can grow through diffusion until they touch one another as is observed in the Ni26CrTi1 steel during the isothermal $\alpha^1 \rightarrow \gamma$ transformation (Fig. 1c).

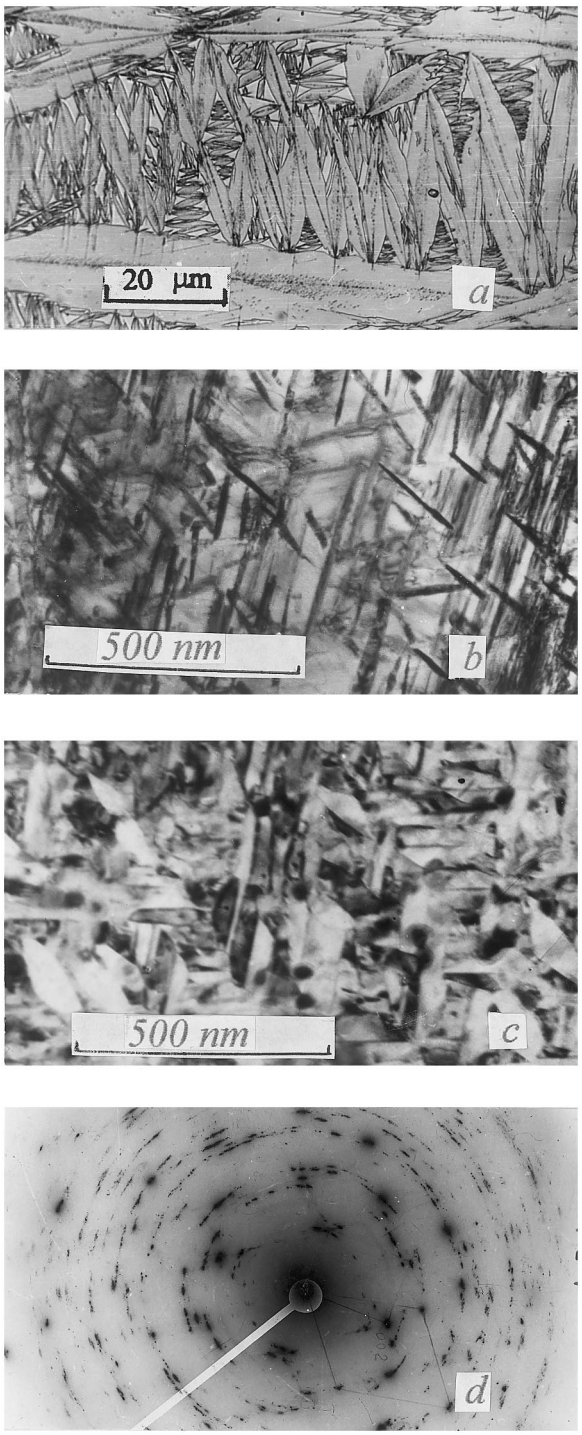

Fig. 1. Initial martensite (a) and nanocrystalline γ-plates formed during $\alpha^1 \rightarrow \gamma$ transformation upon slow heating (0.3 K min^{-1}) to 763 K in the 32Ni alloy (b) and under isothermal conditions (813 K, 2 h) in the 26Ni–Cr–Ti alloy (c); (d) electron diffraction pattern of the structure (c).

3.2. On misorientations of the γ-crystals after the martensitic $\gamma \rightarrow \alpha^1 \rightarrow \gamma$ transformation

A significant property of the ensemble of nanocrystals is the mutual misorientation of any neighboring γ-crystals formed during the martensitic $\gamma \rightarrow \alpha^1 \rightarrow \gamma$ transformation cycle. The ratio between large- and low-angle boundaries of γ-grains may serve as a qualitative indication of the degree of the 'dislocation penetrability' of these boundaries and, correspondingly, of strengthening of the alloy with a superfine grain structure. The total number of possible pairs of γ-crystals among 576 γ-orientations of the 'cycled' austenite is relatively large and equals $576!/574!2! = 165\,600$. However, if the unavoidable multitude of similar misorientations of austenitic crystals is neglected, different misorientations are much less in number. Calculations of the γ-misorientations were performed for the bond matrix of the initial and cycled γ-crystals [7]:

$$H(\varphi) = C_j T^{-1}(\varphi) C_i T(\varphi), \tag{1}$$

where $T(\varphi)$ is the bond matrix of γ- and α^1-lattices after the $\gamma \rightarrow \alpha^1$ transformation; C_i and C_j are matrices describing symmetrical rotations in the cubic lattice, $i(j) = 1, 2, \ldots, 24$; φ is the rotation angle around the rotation axis [3]. The values of the angle φ equal to 0, about 2.63 and about 5.26° correspond to Nishiyama's (N), intermediate (Itm), and Kurdyumov–Sachs' (KS) orientation relationships (OR's), respectively.

From Eq. (1) it follows that in the general case the matrix $H(\varphi)$ has 576 crystallographic variants. One may see however that the values of these matrix elements can change with the value of the subscript i only and should remain unchanged with ascending or descending value of the subscript j, because the matrix C_j is responsible for symmetrical changes in the cubic lattice at the final stage of the transformation, i.e. in the austenite lattice. Therefore, when the value of the subscript j is changed between 1 and 24, fcc crystals will not have new types of orientations except those similar and alike to the orientations that arise with varying value of the subscript i. Thus, crystallographic calculations can give, in the general case, only 24 different types of misorientations of the austenitic crystals formed as a result of the double martensitic $\gamma \rightarrow \alpha^1 \rightarrow \gamma$ transformation relative to one initial crystal. All the other misorientations (determined as $23 \times 24 = 552$) among the total of 576 will be duplicated or prove to be alike. These calculations apply to orientations of all possible 576 austenitic crystals, which are formed after the martensitic $\gamma \rightarrow \alpha^1 \rightarrow \gamma$ transformation cycle, relative to one initial γ-crystal. Obviously, the same is true of all the rest of the 575 crystals, since all the 576 crystallographic variants of the austenitic crystals are equivalent to one another.

All 24 matrices $H(\varphi)$ possible for KS, Itm and N OR's were calculated by Eq. (1). These matrices were used to calculate the angle β and the rotation axes $[U\,V\,W]$ between γ-crystal pairs from the known mathematical formulas:

$$\beta = \arccos\{(h_{11} + h_{22} + h_{33} - 1)/2\}, \tag{2}$$

$$U{:}V{:}W = [h_{12} - h_{21}]{:}[h_{23} - h_{32}]{:}[h_{31} - h_{13}], \tag{3}$$

where h_{ij} stands for the elements of the matrix $H(\varphi)$.

In each particular event calculations were made for 24 different (by the subscript j) crystallographic variants of the matrix $H(\varphi)$ of one specific type (i). The variant with the minimum angle β was chosen. The results of those calculations are given in Table 1. An examination of Table 1 shows that among the calculated 24 typical variants, there were 18 variants for really existing Itm OR's, 17 variants for nearly real KS OR's, and 7 variants for the hypothetical N OR's.

The calculation results obtained for the three types of OR's — with respect to the rotation angle only (disregarding specific rotation axes) and the occurrence rate (or percentage) among the total 24 — are summarized in Fig. 2. From Fig. 2 it is seen that, first, the number of different orientations of the crystals drops with increasing symmetry of OR's and, second, all the misorientations can be divided into two groups with respect to the rotation angle value (Fig. 2): those approximating 'low-angle' misorientations with the angle β ranging between 0 and 21°, and 'large-angle' misorientations having the angle β from 46 to 63°. Mean values of misorientation angles for all possible martensitic OR's cannot be found. One can see (Fig. 2) that large-angle boundaries dominate between γ-crystals formed during the $\gamma \rightarrow \alpha^1 \rightarrow \gamma$ transformation cycle.

It is worth noting that medium-carbon structural steels consist of lath martensite, which groups itself in packets of six martensitic orientations [8] connected with one of the four possible closely packed austenitic planes of the $\{111\}_\gamma$ type. After the martensitic $\gamma \rightarrow \alpha^1$ and $\alpha^1 \rightarrow \gamma$ transformations, when γ-crystals are formed at α^1-boundaries [8], the number of possible austenitic pairs having different misorientations in each martensite packet is limited (only four or five variants). Possible misorientation angles are equal to 0, 60, 57.20, 46.62 and 11.42° for the Itm OR's, and 0, 60, 49.47 and 10.53° for the KS OR's. The other misorientation angles (see Table 1) should be observed between γ crystals at the boundary of martensite packets.

3.3. Variation of the mechanical properties of the alloys in the submicrocrystalline state

The formation of the nanocrystalline structure suggests an improvement of the mechanical properties. It was shown [4,5] that control of the $\alpha^1 \rightarrow \gamma$ transforma-

Table 1
Calculated misorientations of γ-crystals after the $\gamma \rightarrow \alpha^1 \rightarrow \gamma$ transformation by variants (*i*), Kurdjumov–Sachs (KS), intermediate (Itm) and Nishiyama (N) orientation relationship (OR)[a]

Variant No.	KS OR's		Itm OR's		N OR's	
	Angle (°)	Rotation axis	Angle (°)	Rotation axis	Angle (°)	Rotation axis
1	0.00	–	0.00	–	0	–
2	60.00	⟨1.1.1⟩[a]	60.00	⟨1.1.1⟩[a]	60	⟨1.1.1⟩[a]
3	57.21	⟨5.13.15⟩	54.70	⟨4.5.9⟩	19.47	⟨0.1.1⟩
4	20.61	⟨6.11.11⟩	57.23	⟨5.6.8⟩	53.69	⟨16.22.29⟩
5	57.21	⟨3.5.6⟩	55.41	⟨4.6.7⟩	50.05	⟨2.7.7⟩
6	50.51	⟨4.13.16⟩	50.16	⟨2.7.8⟩	50.05	⟨2.7.7⟩
7	50.51	⟨4.13.16⟩	50.16	⟨2.7.8⟩	53.69	⟨16.22.29⟩
8	50.51	⟨2.2.3⟩	52.05	⟨11.13.18⟩	53.69	⟨16.22.29⟩
9	57.21	⟨3.5.6⟩	55.41	⟨4.6.7⟩	13.76	⟨0.0.1⟩
10	14.88	⟨2.12.31⟩	14.05	⟨1.3.16⟩	13.76	⟨0.0.1⟩
11	14.88	⟨2.12.31⟩	14.05	⟨1.3.16⟩	53.69	⟨16.22.29⟩
12	50.51	⟨2.2.3⟩	52.05	⟨11.13.18⟩	62.80	⟨7.17.17⟩
13	10.53	⟨1.1.1⟩	5.26	⟨1.1.1⟩		
14	49.47	⟨1.1.1⟩	54.74	⟨1.1.1⟩		
15	57.21	⟨5.13.15⟩	59.94	⟨3.7.8⟩		
16	21.06	⟨0.4.9⟩	19.88	⟨0.2.3⟩		
17	60.00	⟨0.1.1⟩	57.20	⟨9.10.14⟩		
18	49.47	⟨0.1.1⟩	46.62	⟨0.1.1⟩		
19	51.73	⟨6.11.11⟩	50.75	⟨7.17.17⟩		
20	47.11	⟨3.6.7⟩	50.32	⟨5.8.10⟩		
21	47.11	⟨3.6.7⟩	50.32	⟨5.8.10⟩		
22	20.61	⟨0.5.16⟩	16.95	⟨0.2.13⟩		
23	10.53	⟨0.1.1⟩	11.42	⟨0.2.5⟩		
24	60.00	⟨0.1.1⟩	57.20	⟨9.10.14⟩		

[a] Same as twinning (111).

tion mechanism in the $\gamma \rightarrow \alpha^1 \rightarrow \gamma$ cycle permits the strength characteristics of the metastable Fe–Ni alloys to be significantly enhanced.

The formation of the 15–30% dispersed γ-phase inside martensitic α^1-crystals during the $\alpha^1 \rightarrow \gamma$ transformation, which inhibits movement of dislocations, allows increasing the yield stress $\sigma_{0.2}$ of the 30Ni and 32Ni alloys up to 1150–1050 MPa (Fig. 3), a value which is higher than $\sigma_{0.2}$ of these alloys in the initial austenitic ($\sigma_{0.2} = 250$ MPa) and martensitic ($\sigma_{0.2} = 650$–700 MPa) states. The development of the $\alpha^1 \rightarrow \gamma$ transformation in the α^1-matrix deformed by 80% leads to strengthening of the martensite to 1400 MPa ($\sigma_{0.2}$), which cannot be achieved by plastic deformation of the 30Ni alloy. Plasticity (specific elongation) decreases to 3–7%. Further heating, which causes the appearance of a coarser globular austenite, decreases the strength characteristics almost to the initial level ($\sigma_{0.2} = 350$ MPa) Fig. 3.

Thus, the widely adopted strengthening treatment of structural steels involving the formation of the α^1-martensite in the austenitic matrix by a sharp quenching is replaced in our case by a reverse process, that is, strengthening treatment of the α′-martensite involving the formation of a nanocrystalline austenite in this martensite during heating.

4. Conclusion

It was shown that a nanocrystalline structure with γ-crystals 10–80 nm thick can be produced in austenitic metastable Fe–Ni alloys of the 32Ni and 26Ni–Cr–Ti types as a result of cyclic martensitic $\gamma \rightarrow \alpha' \rightarrow \gamma$ transformations. These transformations give over 500 different γ-orientations in each initial austenitic grain. According to the calculations, large-angle boundaries dominate in the obtained ensemble of austenitic nanocrystals (misorientation angles between neighboring crystals with the KS relationships are 60, 57.7, 57.2, 50.5, 49.5, 47.1, 21.1, 20.6, 14.9, 10.5, and 0°). The strength of the α′-martensite is considerably increased when the nanocrystalline austenite is formed during the reverse martensitic $\alpha' \rightarrow \gamma$ transformation.

Acknowledgements

This study has been supported by the Russian Fundamental Research Foundation (Project No. 96-15-96515).

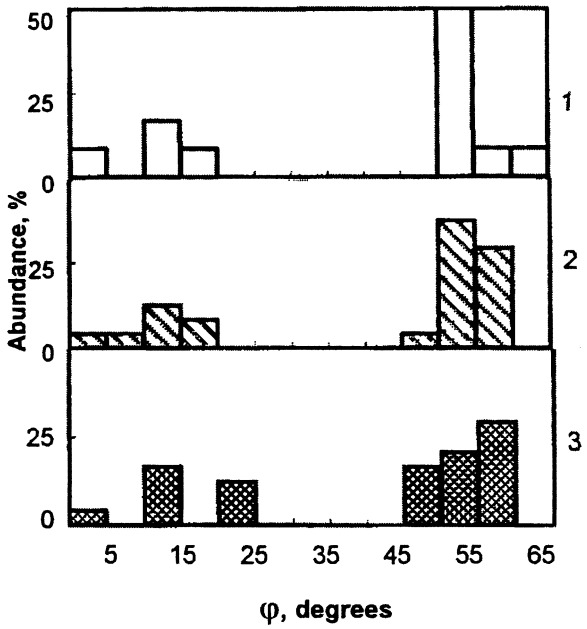

Fig. 2. Bar diagrams showing the distribution of angle misorientations φ austenitic crystals after cyclic fcc→bcc→fcc martensitic transformations for Nishiyama (1), Kurdyumov–Sachs (3) and intermediate (2) orientation relationships.

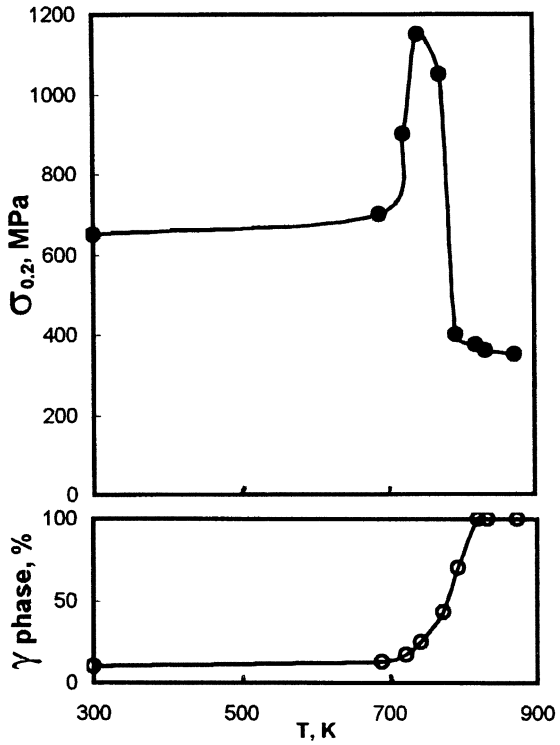

Fig. 3. The yield stress $\sigma_{0.2}$ and amount of austenite γ as a function of temperature during the $\alpha^1 \rightarrow \gamma$ transformation under slow heating (0.3 K min^{-1}). $T_{test} = 298$ K, alloy–Fe–31wt.%Ni.

References

[1] H. Gleiter, Nanostruct. Mater. 6 (1-4) (1995) 3.
[2] V.V. Sagaradze, K.A. Malyshev, Y.A. Vaseva, L.V. Smirnov, Fiz. Met. Metalloved. 37 (1974) 1051.
[3] V.V. Sagaradze, Nanostruct. Mater. 9 (1-8) (1997) 189.
[4] V.V. Sagaradze, Nanostruct. Mater. Sci.Technol. NATO ASI Ser. 50 (3) (1998) 47.
[5] V.V. Sagaradze, A.I. Uvarov, Strengthening of Austenitic Steels, Nauka, Moscow, 1989, p. 270.
[6] V.V. Sagaradze, K.A. Malyshev, V.M. Stchastlivtsev, Y.A. Vaseva, L.M. Proleeva, Fiz. Met. Metalloved. 39 (1975) 1239.
[7] I.P. Sorokin, V.V. Sagaradze, Fiz. Met. Metalloved. 45 (1978) 748.
[8] V.M. Stchastlivtsev, D.P. Rodionov, V.D. Sadovsky, L.V. Smirnov, Fiz. Met. Metalloved. 30 (1970) 1238.